Shoulder Impingement: Objective 3D Shape Analysis of Acromial Morphologic Features[1]

Eric Y. Chang, BS
Daniel A. Moses, MD
James S. Babb, PhD
Mark E. Schweitzer, MD

Purpose: To retrospectively and quantitatively analyze the acromial undersurface in three dimensions and to determine its association with impingement syndrome and rotator cuff tears.

Materials and Methods: Institutional review board approval was received with exemption of informed consent for this retrospective HIPAA-compliant study. Magnetic resonance images were evaluated in 84 patients (63 males, 21 females; mean age, 42.6 years; age range, 15–74 years). On the basis of surgical results, patients were separated into three groups: those without shoulder impingement or rotator cuff tears (31 patients), those with shoulder impingement (22 patients), and those with rotator cuff tears (31 patients). To quantitate the acromial undersurface, the structure was manually plotted, and a mathematic model was created by using splines. The undersurface was divided into a 20×20 grid. For each patient, a shape index (SI) data set and local undersurface angulation (LUA) data set were determined. Regression analyses were used to identify differences between groups, and prediction models were constructed on the basis of correspondent areas.

Results: Analysis of both data sets yielded no apparent progression between groups and demonstrated a lack of similarity between the impingement and rotator cuff tear groups. Discrimination between groups could be demonstrated by dividing the lateral portion of the acromial undersurface into contiguous blocks. The highest overall diagnostic accuracy of our prediction models was 58.3% (49 of 84) by using 10 blocks of the SI data set and 73.8% (62 of 84) by using five blocks of the LUA data set.

Conclusion: Three-dimensional modeling yields objective data about the acromial undersurface. On the basis of this method, osseous impingement by the acromion is not a primary cause of shoulder impingement syndrome or rotator cuff tears.

[1] From the Department of Radiology, New York University Medical Center, New York, NY (E.Y.C., D.A.M., J.S.B., M.E.S.); and Department of Radiology, Hospital for Joint Diseases, New York, NY (M.E.S.). Received February 24, 2005; revision requested April 25; revision received May 23; accepted June 21; final version accepted July 8. **Address correspondence to** E.Y.C., 255 Warren St, Apt 1808, Jersey City, NJ 07302 (e-mail: *eyc212@med.nyu.edu*).

The pathophysiologic cause of rotator cuff disease, and ultimately of rotator cuff tears, is multifactorial, and the relative importance of each component remains debated. Factors intrinsic to the cuff, such as muscle weakness or degenerative tendinopathy and extrinsic compression by soft tissue and bone, are some of the more extensively studied etiologic factors (1–3). Some have suggested that extrinsic osseous impingement is the primary etiologic mechanism of rotator cuff disease and that osseous impingement is related to several causes, such as acquired and often degenerative bone production, congenital and developmental variants in bone shape, and os acromiale (1,4–6).

A major component of osseous impingement is thought to be the morphologic characteristics of the acromion. Consequently, numerous attempts have been made to grade acromial morphologic features. The most notable is the flat (type I), curved (type II), and hooked (type III) classification by Bigliani and colleagues (7), who originally described the acromion by using anatomic specimens. This classification has subsequently been applied to acromia by using multiple imaging modalities. All analyses have been subjective to variable degrees, and significant intraobserver and interobserver variability has been demonstrated (8–10). This interpretive variability is likely the result of several factors, including the subjective nature of nonsystematic interpretation, the artificial demarcation points of the current classification schema, the lack of acknowledgment in the continuum of acromial shapes, the difficulties inherent with uniformly obtaining oblique planes, and the imposition of a two-dimensional construct onto a three-dimensional structure.

Objective quantification of acromial morphologic features is necessary first to determine if this osseous structure is truly associated with the pathogenesis of impingement and second to determine how acromial shape affects the grade or severity of rotator cuff tears. Thus, the purpose of our study was to model and quantitatively analyze the acromial undersurface in three dimensions and to determine its association with impingement syndrome and rotator cuff tears.

Advances in Knowledge

- There is no consistent area of down sloping or convexity in patients with shoulder impingement.
- Osseous impingement by the acromion is not a primary cause of shoulder impingement syndrome or rotator cuff tears.
- Variable origin of the deltoid muscle may be useful in distinguishing between patients with instability, impingement, and rotator cuff tears.

Materials and Methods

Patients

Institutional review board approval with exemption of informed consent was obtained from the New York University Medical Center for this retrospective Health Insurance Portability and Accountability Act–compliant study. Magnetic resonance (MR) images were analyzed in 84 patients (63 males, 21 females; mean age, 42.6 years; age range, 15–74 years) who presented to an orthopedic surgeon for clinical evaluation from 1997 to 2004. All patients who presented to the orthopedic surgeon during this time frame were included in the study, and all had undergone surgery within 14 days of imaging.

On the basis of clinical (eg, range of motion and subacromial injection) and surgical findings, patients were stratified into three groups: The 31 patients who had no evidence of impingement or rotator cuff tear were designated as the instability group, the 22 patients who had shoulder impingement were designated as the impingement group, and the 31 patients who had rotator cuff tears were designated as the rotator cuff tear group. Patient characteristics are shown in Table 1. For the rotator cuff tear group, the length of the tear, the presence or absence of retraction, and the presence or absence of atrophy were characterized for further stratification during final analysis by one author (M.E.S., 15 years of experience in MR imaging of the shoulder) who reviewed each MR image.

Imaging and Data Acquisition

The MR images that were used in this study were obtained by using a 1.5-T MR imager (Symphony/Avanto; Siemens, Erlangen, Germany) with a dedicated shoulder coil. Conventional sagittal oblique spin-echo MR images were used for analysis of the acromion. MR imaging parameters typically consisted of 500–800/10–20 (repetition time msec/echo time msec), a 16-cm field of view, 256 × 256 matrix, 3-mm section thickness, and 0.9-mm intersection gap.

Imaging was performed laterally for the sagittal oblique series, which included images from the first appearance of the acromion, and continued medially until images from the last section through the acromioclavicular joint had been obtained. This ranged from five to eight sections, with a mean and mode of seven sections. The selected Digital Imaging and Communications in Medicine images were exported into Joint Photographic Experts Group format in the original matrix dimension by using DicomWorks (v1.3.5; Puech and Boussel, Lyon, France). For analysis of the left and right shoulders as one group, images of the left shoulders in Joint Photographic Experts Group format were reversed appropriately by using an image

Published online before print
10.1148/radiol.2392050324

Radiology 2006; 239:497–505

Abbreviations:
LUA = local undersurface angulation
SI = shape index

Author contributions:
Guarantor of integrity of entire study, E.Y.C.; study concepts/study design or data acquisition or data analysis/interpretation, all authors; manuscript drafting or manuscript revision for important intellectual content, all authors; manuscript final version approval, all authors; literature research, E.Y.C., M.E.S.; clinical studies, M.E.S.; statistical analysis, E.Y.C., D.A.M., J.S.B.; and manuscript editing, all authors

Authors stated no financial relationship to disclose.

manipulation and graphics program (Photoshop CS; Adobe, San Jose, Calif). Each image series was then imported into a computer-assisted design program (AutoCAD 2005; Autodesk, San Rafael, Calif) while maintaining three-dimensional relationships, such as field of view, section thickness, and intersection gap (Fig 1a).

With the computer-assisted design software, points were used to manually outline the undersurface of the acromion in each section (Fig 1b). The posterior aspect of the acromion was defined at the origin of the deltoid muscle. Any enthesophytes were treated as part of the acromial undersurface and were outlined. On average, 160 points were used for each oblique sagittal series. All points were plotted by a single researcher (E.Y.C.) who was blinded to the group that each patient belonged to. This researcher was trained by another researcher (M.E.S.) over the course of 2 months to recognize and plot the undersurface of the acromion.

Surface Creation and Data Calculation

For each acromion, point data were imported into an interactive mathematics program (Matlab 7.0; Mathworks, Natick, Mass), and the points within each section were interpolated with a one-dimensional spline. Each spline was then resampled so that each section contained the same number of points (Fig 2a). For each acromion, the undersurface was modeled by fitting a two-dimensional smoothing B spline with the Spline Toolbox function (Matlab 7.0; Mathworks) (Fig 2b). B splines belong to a spline curve family that consists of smooth curves defined mathematically by two or more control points and may be used to interpolate or approximate curves and surfaces through multiple points.

The surface was divided into an evenly spaced 20 × 20 grid (400 points), and for each point the magnitude and direction of the two principal curvatures, κ_{min} and κ_{max}, were calculated by using a mathematics program (Matlab 7.0; Mathworks). These curvatures correspond to the minimum (κ_{min}) and maximum (κ_{max}) spatial rates of change for a tangent plane to the surface when moving away from a given point. A detailed mathematic description of splines and principal curvatures is beyond the scope of this article but is outlined in a prior study by one of the authors (11). An informal description of the concept of principal curvatures is reviewed briefly:

As seen in Figure 3, given a surface *S*, a tangent plane *Pt* is constructed to point *p* that lies on *S*. At *p*, **n** denotes a unit vector, which is normal to the tangent plane. A second plane (*Po*) is constructed that contains **n**, which is orthogonal to the tangent plane. As this second plane is rotated 180° around the normal vector **n**, an infinite number of curvatures will arise from the intersection (surface curve) between *S* and the rotating plane. Where these curves intersect at *p*, the curvature (κ) will demonstrate more curve at larger values and opposite curve depending on the sign. A κ of 0 would denote a straight line segment. If κ_{max} is equal to κ_{min} but not equal to zero, then the local section of the surface is purely concave or convex. Our example in Figure 3 demonstrates a purely convex surface.

From the two principal curvature

Table 1

Patient Characteristics

Group	No. of Patients	Mean Age (y)	Age Range (y)	Left Shoulder	Right Shoulder
Instability					
Female	4	28	20–41	3	1
Male	27	30	15–52	10	17
Impingement					
Female	9	47	31–56	4	5
Male	13	51	40–74	9	4
Rotator cuff tear					
Female	8	57	31–69	2	6
Male	23	48	23–71	12	11

Figure 1

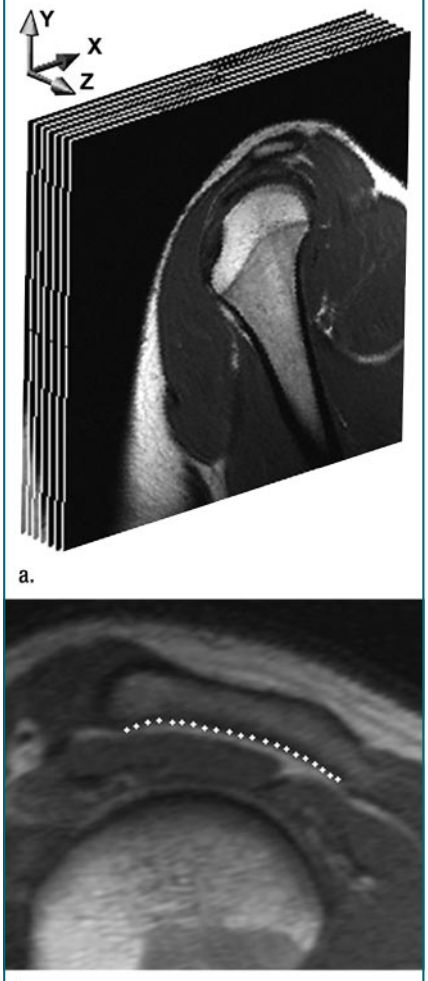

Figure 1: **(a)** Seven sagittal oblique spin-echo MR images (688/14, 16-cm field of view, 256 × 256 matrix, 3-mm section thickness, 0.9-mm intersection gap) imported into a three-dimensional space, with 3.9-mm spacing between each image. **(b)** Sagittal oblique T1-weighted spin-echo MR image (783/13, 16-cm field of view, 512 × 512 matrix, 3-mm section thickness) demonstrates example of points along acromion undersurface. Figure is used only as an example; actual points for data analysis were at pixel level and were not easily visualized.

values we can determine the shape index (SI), which is a convenient mathematic method to provide a local shape description. At each of the 400 points, SI was calculated by using a mathematics program (Matlab 7.0; Mathworks) and was defined as follows: $-2/\pi \tan^{-1}[(\kappa_{max} + \kappa_{min})/(\kappa_{max} - \kappa_{min})]$. SI values range from −1.0 to 1.0, with negative indices indicating a concave shape and positive indices indicating a convex shape (Fig 4). SI provided us with our first data set for analysis, which contained 400 values for each of the 84 patients.

Additionally, the relative angulation of the normal vector at each of the 400 points was measured with the same mathematics program (Matlab 7.0; Mathworks). First, normal vectors, $\mathbf{n}_{s(u,v)}$, were calculated at each of the 400 points along the acromial undersurface (Fig 5a). We then created a plane of best fit through the resampled points of the acromial undersurface and determined the normal vector $\mathbf{n}_{plane}$ of this plane. At each point along the 20 × 20 grid we calculated the angle difference as the absolute value of these two vectors, $\mathbf{n}_{plane} - \mathbf{n}_{s(u,v)}$ (Fig 5b). We refer to this as the local undersurface angulation (LUA). This provided us with a second data set for analysis that also contained 400 values for each of the 84 patients. This data set provided an absolute value and did not indicate direction (as is the case in an upward- or downward-sloping section), so we also obtained the relative component in the magnet coordinate z-axis.

Statistical Analysis

Two data sets, each containing 33 600 entries (84 patients, 400 points), were created from the output values as outlined in the previous section—one set was created for SI and the other was created for LUA. For each data set, patients were categorized into three mutually exclusive groups (shoulder instability, impingement, or rotator cuff tear), and analyses were conducted in two stages.

The first stage was used to identify blocks of contiguous data points that exhibited differences between patient groups after adjusting for age and sex. For this, we used an analysis of variance as a filter to identify a reasonably small number of shoulder locations that could be used for a more formal second stage of analysis. Each separate analysis of variance used only a single observation (SI or LUA at a specific shoulder location) for each patient; therefore, no intrapatient correlations needed to be accounted for. Type III *P* values, which were used to assess the difference between diagnosis groups with respect to SI and LUA at each location (adjusted for age and sex), were employed as a mechanism for ranking each point along the acromial undersurface so that a subset of data could be selected for the subsequent analyses. Consequently, the first stage produced a set of data blocks that represented contiguous regions of the shoulder where SI or LUA seemed to exhibit an association with the diagnosis.

The second stage of analysis was based on logistic regression, and diag-

Figure 2

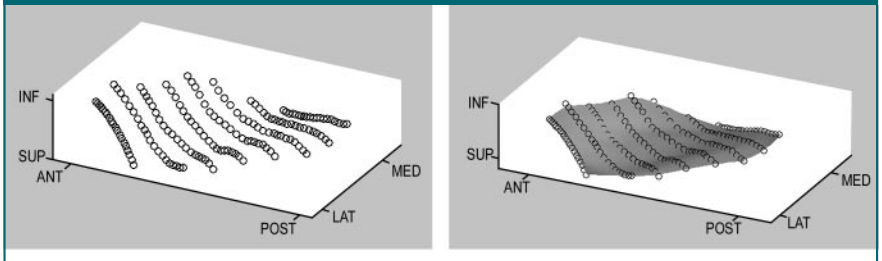

a. **b.**

Figure 2: **(a)** Resampled points along acromial undersurface for each MR section. **(b)** Undersurface of acromion reconstructed from points in **a** by using B splines. *ANT* = anterior, *INF* = inferior, *LAT* = lateral, *MED* = medial, *POST* = posterior, *SUP* = superior.

Figure 3

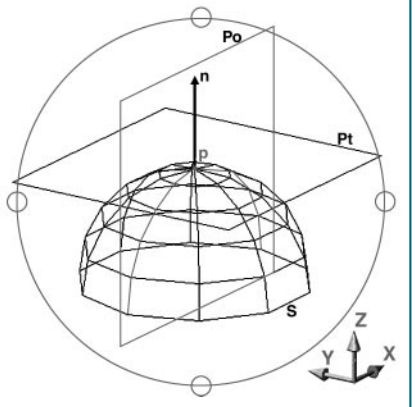

Figure 3: Surface *S* with tangent plane *Pt* at point *p*. Plane *Po* is orthogonal to tangent plane *Pt*. Curvature *k* arises from surface *S* as *Po* is rotated about vector **n**.

Figure 4

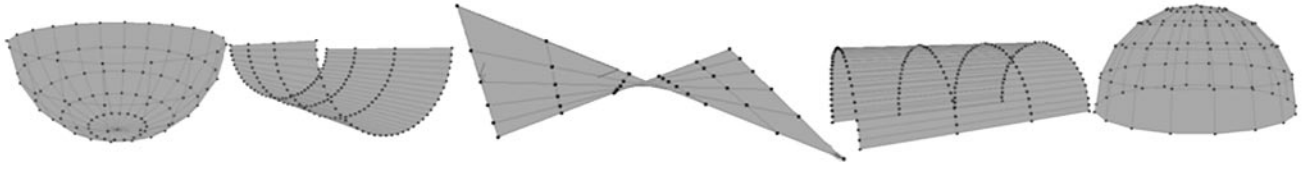

Figure 4: Graphic representation of SI for (right to left) −1.0 concave, −0.5 rut, 0.0 saddle, 0.5 ridge, and 1.0 convex shapes.

Figure 5

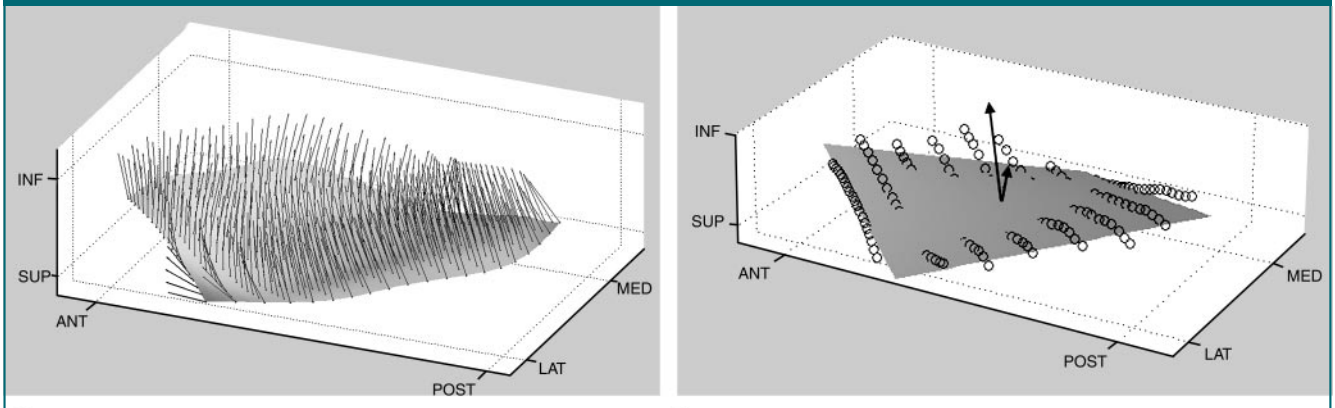

a. b.

Figure 5: **(a)** Normal vectors at each point on 20 × 20 grid along acromial undersurface. **(b)** Plane of best fit through resampled points demonstrates LUA, which was defined as a normal vector of the acromial undersurface in **a** (longer arrow) subtracted from normal vector of plane (shorter arrow). *ANT* = anterior, *INF* = inferior, *LAT* = lateral, *MED* = medial, *POST* = posterior, *SUP* = superior.

nosis was used as a dependent variable for each patient. Because of the vast quantity of data, the mean value of SI or LUA within each block of data was used to construct diagnostic prediction models with ordinal (order assumed for instability, impingement, and cuff tear), nominal (no order assumed for instability, impingement, and cuff tear), and binary (presence vs absence of each condition) logistic regression analyses.

Additionally, the mean value for each point along the acromial undersurface was examined for comparison between the three groups, and relationships between the length of the tear, the presence or absence of retraction, and the presence or absence atrophy were compared. Receiver operating characteristic curves were used to assess the diagnostic utility of mean SI and LUA assessments for each specific condition (instability, impingement, or rotator cuff tear). A statistician (J.S.B.) performed all statistical computations by using a commercially available software program (SAS for Windows, version 9.0; SAS Institute, Cary, NC).

Results

In the rotator cuff tear group, the mean length of the tear was 1.1 cm (range, 1 mm to 4 cm). Of the 31 patients in this group, 25 had no retraction or atrophy, two had retraction and atrophy, one had atrophy and no retraction, and three had retraction and no atrophy.

Analysis of SI

It was observed that neither age nor sex was significantly associated with SI. By using an analysis of variance, we were unable to identify portions of data that exhibited significant differences ($P < .05$) between patient groups. We identified 10 blocks of contiguous data that exhibited trends ($.05 < P < .1$), and a graphic overlay onto an acromial undersurface was created (Fig 6). By using the average SI for each of the 10 blocks, we were able to show the results of the ordinal logistic regression and nominal logistic regression (Table 2). The prediction models that were based on average SI exhibited a high propensity for misdiagnosis in patients with impingement. For both regression analyses, however, the highest sensitivity was found for diagnosis in the shoulder instability group.

Analysis of LUA

By using the mean LUA value for each point, we created a graphic overlay onto an acromial undersurface for all three groups (Fig 7). Of note, the lateral edge for the impingement group had an overall greater LUA than the lateral edge for the instability or rotator cuff tear group. This relationship remained even after stratifying the rotator cuff tear group according to the length of the tear, the presence or absence of retraction, and the presence or absence atrophy. From the magnet coordinate z-axis compo-

Figure 6

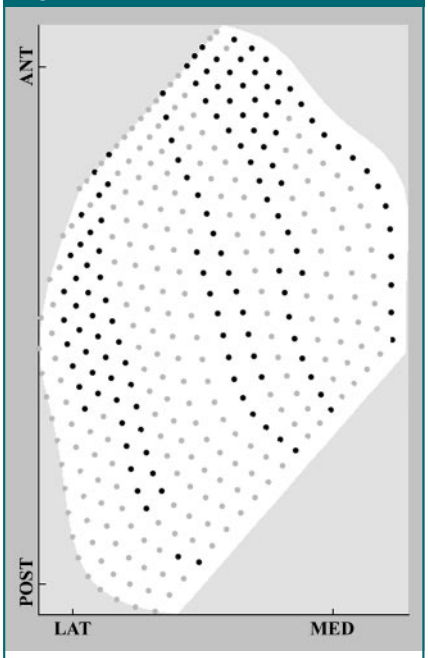

Figure 6: Blocks of contiguous data overlaid onto an acromial undersurface demonstrate a trend to distinguish between patient groups, as determined by *P* value ($.05 < P < .1$) on the basis of SI. *ANT* = anterior, *LAT* = lateral, *MED* = medial, *POST* = posterior.

nent, it was shown that greater LUA in this area was caused by the upward sloping of the lateral edge.

It was observed that neither age nor sex was significantly associated with LUA. *P* values that were calculated from the analysis of variance on the LUA data set were used to create a graphic overlay onto an acromial undersurface (Fig 8a). On the basis of these results, attention was focused on the data points that corresponded to the lateral portion of the acromion; this area contained the majority of significant values ($P < .05$) and has been described in the literature as being a risk factor for impingement (7,12). Diagnostic prediction models were constructed on the basis of the mean value of the LUA within each of five spatially contiguous blocks (Fig 8b). Only nominal logistic regression was performed because we were unable to unambiguously discern an ordering for the three groups. In particular, while the impingement group had a higher mean value for the LUA in each of the five blocks, the relative order of the shoulder instability group and rotator cuff tear group varied from block to block (Table 3).

In all subsets, variable selection was used to identify the two diagnostic models that exhibited the best performance in terms of overall diagnostic accuracy (Table 4). The first model used only the mean measurements from blocks 3, 4, and 5, while the second model used the

Table 2

Results Obtained by Using Average SI in 10 Blocks for Diagnosis

True Diagnosis	Predicted Diagnosis: Instability	Impingement	Rotator Cuff Tear	Sensitivity (%)*
	Ordinal Logistic Regression†			
Instability	25	0	6	80.6 (25/31)
Impingement	12	0	10	0 (0/22)
Rotator cuff tear	10	0	21	67.7 (21/31)
	Nominal Logistic Regression‡			
Instability	21	6	4	67.7 (21/31)
Impingement	7	8	7	36.4 (8/22)
Rotator cuff tear	9	2	20	64.5 (20/31)

* Numbers in parentheses were used to calculate percentages.

† Overall diagnostic accuracy was 54.8% (46 of 84).

‡ Overall diagnostic accuracy was 58.3% (49 of 84).

Figure 7

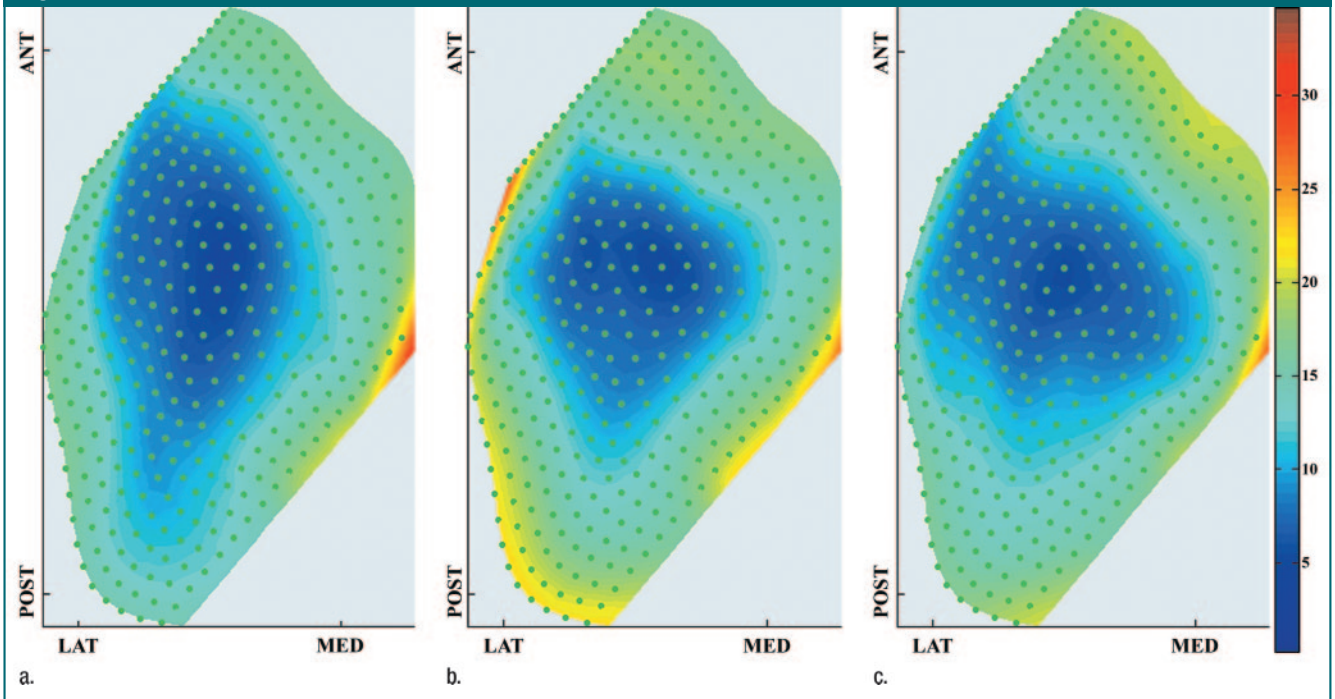

Figure 7: Mean value of LUA at each point on 20 × 20 grid overlaid onto acromial undersurface with color bar for **(a)** instability group, **(b)** impingement group, and **(c)** rotator cuff tear group. Note that the lateral edge in **b** has an overall greater angulation than the lateral edge in **a** or **c**. *ANT* = anterior, *LAT* = lateral, *MED* = medial, *POST* = posterior.

mean measurements from all five blocks in addition to patient age.

Receiver operating characteristic curves were generated for the three diagnostic models for this data set, and the areas under the curve were calculated as 0.952 for the instability group, 0.833 for the impingement group, and 0.844 for the rotator cuff tear group (Fig 9).

Discussion

In 1972, Neer (1) described subacromial impingement syndrome as a distinct entity on the basis of clinical observations and cadaveric scapulae dissection. He proposed that the rotator cuff was impinged on by the anterior one-third of the acromion, by the coracoacromial ligament, and by the acromioclavicular joint. Furthermore, Neer focused on the shape of the anterior acromial undersurface and concluded that variations in the undersurface, such as an overhanging curve or spur, were in part responsible for subacromial impingement and associated rotator cuff tears. In several later studies, acromial undersurface shape was found to have a relationship to rotator cuff disease (12–15).

Many have questioned, however, the reliability of current classification systems. Zuckerman et al (8) demonstrated a poor to fair level of interobserver reliability by using anatomic specimens with the classification system of Bigliani and colleagues (7). Peh et al (10) found that apparent acromial shape varied on supraspinatus muscle outlet radiographs depending on minor variations in angulation and that apparent acromial shape varied on MR images depending on the acquisition of lateral versus more medial sections. In another study, Jacobson et al (9) reviewed 126 supraspinatus outlet radiographs and found good to excellent intraobserver reliability but fair interobserver reliability at best. On the basis of their results, Jacobson and colleagues concluded that a system that incorporates more objective classification criteria and acknowledges the continuous nature of acromial morphologic types may improve reliability and validate the use of the classification system for making clinical and surgical judgments (9).

On the basis of the systematic and quantitative methods used in our study, our results are similar to those of previous studies in that they indicate the acromial undersurface to be useful in distinguishing between groups of patients who demonstrate instability, impingement, or rotator cuff tears. These results, however, are not based on a single summary statistic but rather on 10 summary SIs or at least three summary LUA values.

Our results suggest that there is not a simple progression of acromial shapes between patients with instability, impingement, or rotator cuff tears. Furthermore, although each group is distinguishable with our LUA statistical prediction model, the lateral acromial edge of the group with shoulder instability is more similar to that of the group with rotator cuff tears, and both groups appear different from the impingement group. This relationship remained even after reviewing each case within the rotator cuff tear group and stratifying patients according to the length of the

Figure 8

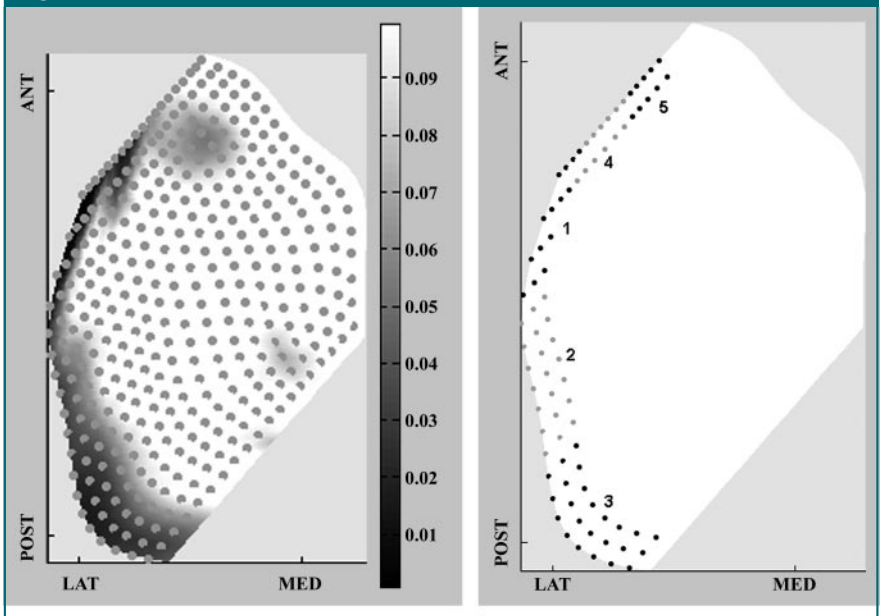

a. b.

Figure 8: **(a)** *P* values calculated from an analysis of variance on the basis of LUA data set. Graphic overlay onto acromial undersurface demonstrates that the majority of significant values ($P < .05$) are within the lateral portion. **(b)** Diagnostic model built on the basis of the mean value of each of these five spatially contiguous blocks. *ANT* = anterior, *LAT* = lateral, *MED* = medial, *POST* = posterior.

Table 3

Mean Value of LUA in Five Contiguous Summary Blocks

Block	Instability Group	Impingement Group	Rotator Cuff Tear Group
1	26	37	22
2	27	32	24
3	24	35	30
4	20	27	18
5	21	29	26

tear, the presence or absence of retraction, and the presence or absence of atrophy. Interestingly, this corresponding area was not down sloping or hooked but rather up sloping. We were unable to distinguish any consistently down-sloping area in the impingement group, and our results lead us to believe that subacromial impingement syndrome and rotator cuff tears are not caused by primary extrinsic osseous impingement.

Figure 9

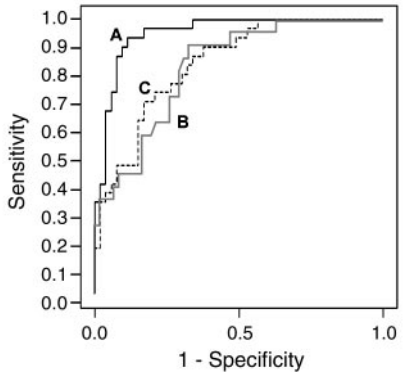

Figure 9: Receiver operating characteristic curves for the binary prediction models generated from the mean local undersurface angulation in five blocks to diagnose each specific condition. Area under the curve is 0.952 for instability (*A*, black line), 0.833 for impingement (*B*, gray line), and 0.844 for rotator cuff tears (*C*, dotted line).

The results of our study provide a partial response to the controversy surrounding the cause of rotator cuff disease. Other proposed intrinsic mechanisms, such as primary degeneration (possibly vascular and ischemic in nature) of the cuff or overuse, may play more important roles (16,17). Our data show that the lateral edge of the acromion remains potentially useful in diagnosis, although the mechanism does not appear to be through osseous impingement. The lateral edge of our three-dimensional undersurface model corresponds to the posterior aspect of the individual sagittal oblique sections. Our plotting technique defined the true edge of the acromion at the origin of the deltoid muscle. This raises the possibility that the point of deltoid origin may have a primary or secondary role in subacromial impingement syndrome and rotator cuff tears.

LUA, which had an overall diagnostic accuracy of 73.8% (62 of 84), appears to be much more useful than SI, which had an overall diagnostic accuracy of 58.3% (49 of 84). We believe this difference is partly the result of limitations in using SI for our analysis. While theoretically useful for determining the concavity and convexity of a local point, SI does not indicate the absolute amount of osseous narrowing. An illustrative example is an acromion with a constant mildly convex surface that begins medially and extends laterally. Numerically speaking, SI at each individual point on the acromial undersurface would not capture the total amount of narrowing at the lateral edge. Additionally, any combination of convex points could lead to the same outlet narrowing, thereby making it difficult to compare specific points across acromia. This is where the LUA proves more useful in that it provides the relative degree of angulation at a specific point.

There are additional limitations to the shape analysis technique used in this study. One shortcoming lies in the statistical analysis. With regard to ordinal logistic regression, our analysis did not assume a proportional odds model. This may be a confounding factor leading to poor performance, aside from the suggestion that there is no progression between groups.

Additionally, an intrinsic shortcoming of shape analysis lies in the technical difficulty of comparing vastly different shapes to one another. Along these lines, in an analysis for which a specific location on an anatomic structure is compared across patients, there is a direct relationship between the size of the grid used to divide the structure (total number of points) and the amount of misregistration. For two differently shaped acromia that are both divided into 20×20 grids, each point does not anatomically correlate as well between patients as each point on a 5×5 grid. For our study, we attempted to minimize misregistration and maintain relative anatomic accuracy between the acromia of patients by using summary statistics and the fact that the acromial undersurface is smooth and continuous in shape. Also important when recreating a structure is the use of thin sections. In particular, we noticed occasional degradation of cortical resolution on the most lateral section of the acromion because of volume averaging.

The use of a minimal intersection gap was also an important factor. We were able to accurately plot the surface within the plane of each section, but there were fewer control points for two-dimensional smoothing B splines when moving between sections. With regard to the latter problem, one could plot

Table 4

Results of Nominal Logistic Regression by Using Mean LUA for Diagnosis

True Diagnosis	Predicted Diagnosis: Instability	Impingement	Rotator Cuff Tear	Sensitivity (%)*
	Blocks 3, 4, and 5†			
Instability	24	0	7	77.4 (24/31)
Impingement	2	10	10	45.5 (10/22)
Rotator cuff tear	4	4	23	74.2 (23/31)
	Blocks 1–5 and Patient Age‡			
Instability	26	0	5	83.9 (26/31)
Impingement	1	13	8	59.1 (13/22)
Rotator cuff tear	4	4	23	74.2 (23/31)

* Numbers in parentheses were used to calculate percentages.

† Overall diagnostic accuracy was 67.9% (57 of 84).

‡ Overall diagnostic accuracy was 73.8% (62 of 84).

points in at least two imaging planes and superimpose the points in three-dimensions (multiplanar reconstruction).

In conclusion, our results do not support the previous thinking that osseous impingement by any portion of the acromion leads to subacromial impingement syndrome. Additionally, there is a lack of continuum between acromial morphologic features and progression to tear, which suggests that osseous impingement is not primarily responsible for rotator cuff tears. Intrinsic shape determination of the acromial undersurface by using the technique proposed in this study has the potential to distinguish between patients with instability, impingement, or rotator cuff tears, possibly because of the variable origin of the deltoid muscle. We believe that the technique for shape analysis that is used in this study demonstrates promise and provides a baseline for future projects in which the concept of shape interaction aids in the understanding of musculoskeletal disorders.

References

1. Neer CS 2nd. Anterior acromioplasty for the chronic impingement syndrome in the shoulder: a preliminary report. J Bone Joint Surg Am 1972;54:41–50.
2. Ogata S, Uhthoff HK. Acromial enthesopathy and rotator cuff tear: a radiologic and histologic postmortem investigation of the coracoacromial arch. Clin Orthop Relat Res 1990;254:39–48.
3. Nirschl RP. Rotator cuff tendinitis: basic concepts of pathoetiology. Instr Course Lect 1989;38:439–445.
4. Yazici M, Kopuz C, Gulman B. Morphologic variants of acromion in neonatal cadavers. J Pediatr Orthop 1995;15:644–647.
5. Nicholson GP, Goodman DA, Flatow EL, Bigliani LU. The acromion: morphologic condition and age-related changes—a study of 420 scapulas. J Shoulder Elbow Surg 1996;5:1–11.
6. Hutchinson MR, Veenstra MA. Arthroscopic decompression of shoulder impingement secondary to os acromiale. Arthroscopy 1993;9:28–32.
7. Bigliani LU, Morrison DS, April EW. The morphology of the acromion and its relationship to rotator cuff tears. Orthop Trans 1986;10:216.
8. Zuckerman JD, Kummer FJ, Cuomo F, Greller M. Interobserver reliability of acromial morphology classification: an anatomic study. J Shoulder Elbow Surg 1997;6:286–287.
9. Jacobson SR, Speer KP, Moor JT, et al. Reliability of radiographic assessment of acromial morphology. J Shoulder Elbow Surg 1995;4:449–453.
10. Peh WC, Farmer TH, Totty WG. Acromial arch shape: assessment with MR imaging. Radiology 1995;195:501–505.
11. Moses DA, Axel L. Quantification of the curvature and shape of the interventricular septum. Magn Reson Med 2004;52:154–163.
12. MacGillivray JD, Fealy S, Potter HG, O'Brien SJ. Multiplanar analysis of acromion morphology. Am J Sports Med 1998;26:836–840.
13. Toivonen DA, Tuite MJ, Orwin JF. Acromial structure and tears of the rotator cuff. J Shoulder Elbow Surg 1995;4:376–383.
14. Morrison DS, Bigliani LU. The clinical significance of variations in acromial morphology. Orthop Trans 1987;11:234.
15. Epstein RE, Schweitzer ME, Frieman BG, Fenlin JM Jr, Mitchell DG. Hooked acromion: prevalence on MR images of painful shoulders. Radiology 1993;187:479–481.
16. Codman EA. Rupture of the supraspinatus. J Bone Joint Surg 1937;19:643–652.
17. Jobe FW, Kvitne RS, Giangarra CE. Shoulder pain in the overhand or throwing athlete: the relationship of anterior instability and rotator cuff impingement. Orthop Rev 1989;18:963–975.